TISSUE ENGINEERING: Part C
Volume 15, Number 3, 2009
© Mary Ann Liebert, Inc.
DOI: 10.1089/ten.tec.2008.0485

Generation of Functional Neural Artificial Tissue from Human Umbilical Cord Blood Stem Cells

Marcin Jurga, Ph.D.,[1] Andrzej W. Lipkowski, Ph.D.,[2,3] Barbara Lukomska, Ph.D.,[1] Leonora Buzanska, Ph.D.,[1,4] Katarzyna Kurzepa, Ph.D.,[3] Tomasz Sobanski, Ph.D.,[4] Aleksandra Habich,[1] Sandra Coecke, Ph.D.,[4] Barbara Gajkowska, Ph.D.,[5] and Krystyna Domanska-Janik, Ph.D., M.D.[1]

Stem cell–based regenerative neurology is an emerging concept for treatment of diseases of central nervous system. Among variety of proposed procedures, one of the most promising is refilling of cystic cavities of injured brain parenchyma with artificial neural tissue. Recent studies revealed that after allogenic transplantation in rodents these tissue-engineered entities were shown efficient in repair of hypoxic/ischemic brain injury. Human umbilical cord blood (HUCB) was recognized to be an efficient and noncontroversial source of neural stem cells (NSC). The main purpose of this study was to generate HUCB-derived neural artificial tissue and investigate their functional properties. Neural organoids formed on human-originated biodegradable scaffolds within 3 weeks and resembled niche structure where immature stem cells (Oct4+ and Sox2+) and proliferating neuroblasts (Nestin+, GFAP+, and Ki67+) were present. Such aggregates were placed on multi-electrode chips and differentiated toward mature neurons (TUJ1+ and MAP2+). These three-dimensional aggregates in contrast to two-dimensional cultures formed functional circuits and generated spontaneous field/action potentials. Our results indicate that three-dimensional environment facilitates maturation of HUCB-derived NSC what should be considered regarding regenerative medicine application.

Introduction

The central nervous system (CNS) has limited self-repair capabilities. Neural stem cells (NSC), though existing in the adult brain, are not robust enough to promote a functional and stable recovery of CNS after its structural lesions.[1] For this reason, stem cell–based therapy might in the near future come to represent a plausible alternative strategy applicable to neurological disorders. In animal models, different cellular transplantation strategies have shown some efficacy where the treatment of various types of CNS injuries is concerned.[2–4] Direct brain transplantation, as well as intravenous, intraarterial, or selective endovascular infusion, remains potential avenues for stem cell delivery. Transplanted cells are either committed to the required cell type before application or applied directly, without prior differentiation, in line with the concept that signals in the host tissue will induce their differentiation *in situ*.[5] *In vivo* experiments have demonstrated migratory properties of these cells and their capacity to maintain multipotency within the host brain, albeit a long-term survival of individual cells still remains rather elusive.[6,7] Survival of transplanted stem cells and their proliferation and differentiation properties are partially limited by the histocompatibility between donor and recipient, but strongly depend on local microenvironment upon transplantation. A neural loss that follows brain stroke often effects in cystic cavities within brain parenchyma. Such lesion is physically separated from surrounded tissue, and no solid extracellular matrix (ECM) proteins are present within to serve as a scaffold for migrating neuroblasts. Therefore, current therapeutic strategies based on grafting of SC suspension out of the lesion site might not be ideal to refill such cavities. An alternative strategy proposes transplantation of artificial tissue based on biodegradable scaffolds. Such three-dimensional (3D) scaffold–based artificial neural tissue can be tailored to the lesion size according to MRI scanning results and delivered directly into the cavity. Moreover, artificial tissue based on biodegradable supporting material is supposed to be more resistant to the transplantation stress than dispersed stem

[1]Department of Neurorepair, Medical Research Institute, Polish Academy of Sciences, Warsaw, Poland.
[2]Department of Neuropeptide, Medical Research Institute, Polish Academy of Sciences, Warsaw, Poland.
[3]Industrial Chemistry Research Institute, Warsaw, Poland.
[4]Institute for Health and Consumer Protection, JRC, European Commission, Ispra, Italy.
[5]Department of Cell Ultrastructure, Medical Research Institute, Polish Academy of Sciences, Warsaw, Poland.

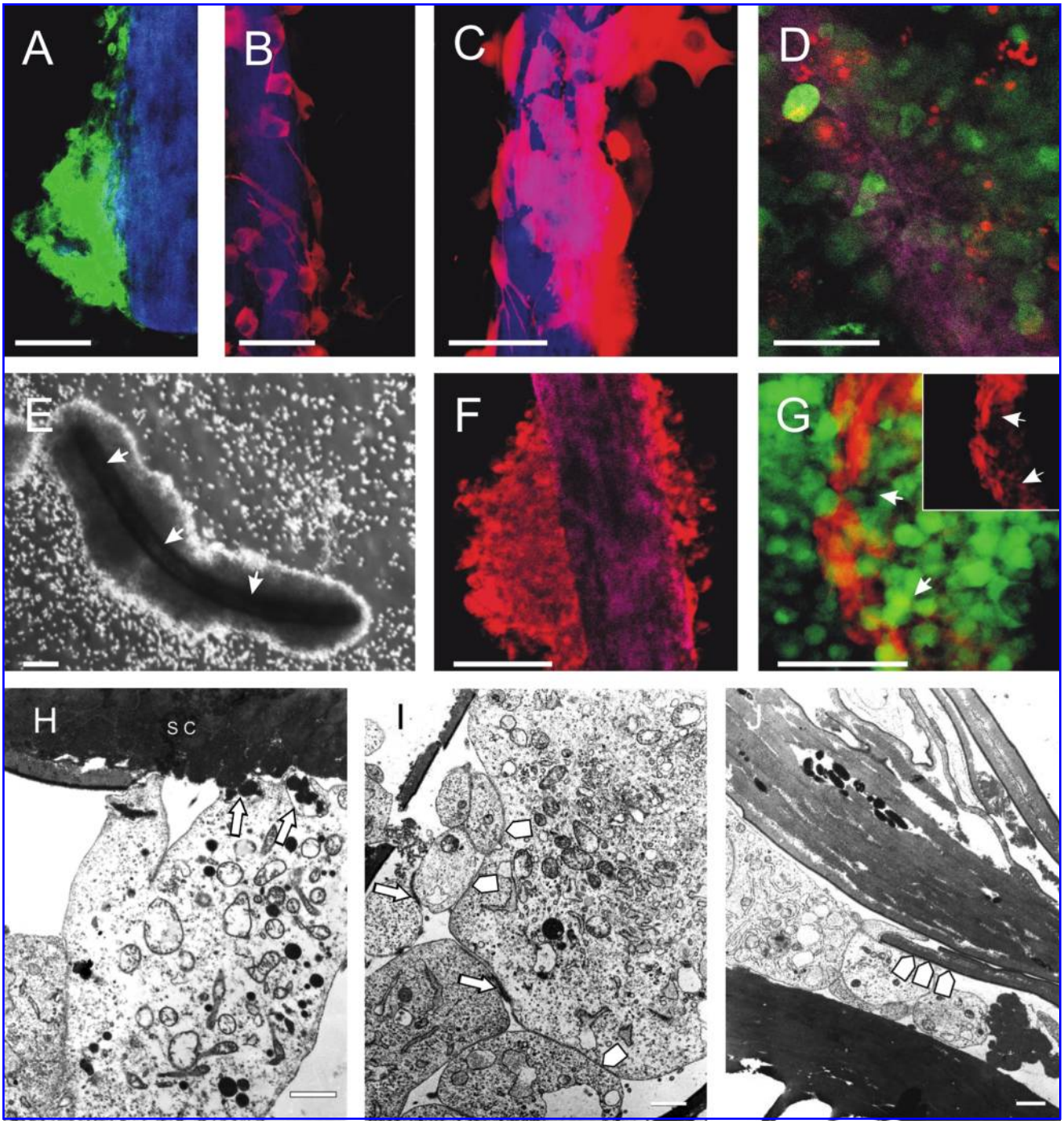

FIG. 1. Neural niche–like aggregates based on biodegradable scaffolds derived from HUCB stem cells. During formation of the aggregate, different types of neural cells are present on the HKAP scaffold: (**A**, green) neuroblasts [NF200+], (**B**, red) neurones [MAP2+], (**C**, red) astrocytes [S100β+], and (**D**, red) proliferating cells [Ki67+]. The HKAP scaffold is located at the center of mature aggregate (**E**). HKAP scaffolds were labeled blue (**A–C**), purple (**D, F**), and red (**G**). HUCB-NSC were additionally labeled by green cell tracker to visualize cell bodies penetrated inside the HKAP scaffolds (**D, G**). HKAP scaffolds were digested by penetrating stem cells (**G**, inset; arrows indicate the digested regions within the HKAP). TEM microphotographs show endocytosis (**H**, arrows) and phagocytosis (**J**, arrowheads) of digested scaffolds [SC] by NSC. Confocal scanning through the center of mature aggregate of HUCB-NSC revealed expression of connexin 43 [red] grown around HKAP scaffold (**F**). TEM microphotographs show gap junction (**I**, arrowheads) and tight junction (**I**, arrows) between the HUCB-NSC in the core of aggregate and very tight connection of HUCB-NSC to the HKAP (**J**). Scale bars: (**A–G**) 50 μm; (**H–J**) 1 μm.

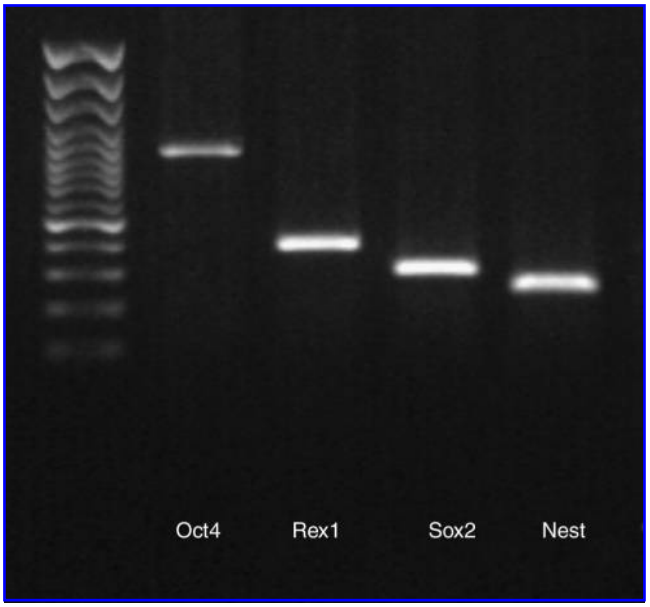

FIG. 2. RT-PCR analysis of mRNA expression by NSC niche–like aggregates derived from HUCB. Cells maintained in serum-free medium (containing EGF) as free-floating aggregates express genes characteristic for pluripotent stem cells: *Oct4*, *Sox2*, and neural development *Rex1*, and Nestin (*Nest*).

cells. Study performed by Snyder group claimed that allogenic transplantation in mice of scaffold-based neural cells was shown efficient in repair of hypoxic/ischemic brain injury.[8]

The assumption underpinning the research that our group carried out was to establish a culture system of functional artificial neural tissue for their application in regeneration of CNS lesions. To generate artificial brain tissue, we used human umbilical cord blood–derived neural stem cells line (HUCB-NSC) seeded on biodegradable scaffolds of human origin produced with nonimmunogenic keratin-associated protein (HKAP). We have decided to use cord blood cells, which have been an element of clinical practice for over 20 years in hematological disorders and offering several advantages in regard of clinical transplantation. Neurogenic potential of SC derived from cord blood has been already described by number of groups.[9,10] HUCB stem cells have been used already as in single clinical trial for regeneration of damaged spinal cord.[11] The HUCB-NSC generated recently in our laboratory is nontransformed cell line that grows continuously in culture. These cells maintain their growth rate and the ability to differentiate into neuronal-, astrocyte-, and oligodendrocyte-like cells.[12,13] HUCB-NSC retains as well the pool of undifferentiated cells expressing markers of pluripotency (*Oct4*, *Sox2*, and *Nanog*).[12] Moreover, what is of high importance, transplantation of HUCB-NSC into immunodeficient NOD/SCID mice has never evoked tumors in contrast to embryonic and induced pluripotent stem cells. Functional human neuronal cells have already been generated from embryonic SC.[14] Our studies show that 3D scaffold–based aggregates derived from HUCB-NSC can be differentiated *in vitro* to the level enabling them to form neuronal network generating spontaneous electric field potentials being a function of active action potentials. We found in this study that 3D environment supporting proper cell–cell interactions through gap and tight junction connections is crucial for gaining functional properties by neuronal circuits. Results presented here indicate that HUCB can serve as safe, efficient, and ethically sound source of stem cells for neural tissue engineering.

Materials and Methods

Cell culture protocol

NSC line derived from HUCB-NSC[13] was cultured in serum-free medium: DMEM/F12 supplemented with B27 (1:50; all from Gibco, Paisley, UK), EGF (20 ng/mL; Sigma, Manchester, UK), and antibiotic–antimycotic solution (1:100; Sigma) in a density of 0.1–0.5 million cells/mL. HKAP scaffolds have been added to cell culture (approximately 50 scaffolds per bottle [25 cm^2]). Scaffolds were preparated by the method already patented.[15] HKAP scaffolds were prepared by removing enzymatic digestible material from partitioned human hair through a combination of chemical activation and proteolytic enzymatic digestion. Briefly, nonchemically treated hair donated by a white male was activated with sodium hydroxide, washed with water, and digested with pepsin. Solid residue was washed with water, dried, and grounded to small (<0.2 mm) fragments. Then, solid material was digested again with pepsin, washed with water, and dried. The shape of the scaffolds can be easily modified during melting stage what *ipso facto* determine the size of the aggregates. Cultures were maintained in air with 5% CO_2 and 95% humidity at 37°C. The cells were fed every 3–4 days. Within the first week of culture in defined, serum-free medium, single cells were attaching equally all over the surface of floating HKAP scaffolds. Subsequently, during the next 7 days of culture the NSC formed local 3D colonies around the centrally situated HKAP scaffold. At the third week of culture these local colonies (niches) joined each other and created a uniform 3D aggregate of NSC with protein scaffold placed in their core. When the aggregate reaches maximum size (approximately 300 μm thickness of cell layer measured from the central scaffold to the aggregate surface), their growth was inhibited without any signs of necrosis in the core of the aggregate. Adult, floating aggregates may be maintained *in vitro* for several weeks without significant changes in their morphology, their potential to differentiation, and with no observed apoptosis. However, in time the internally situated scaffold is digested by surrounded cells that simultaneously penetrate inside the scaffold.

Differentiation protocol

Aggregates of NSC derived from HUCB-NSC that grow based on HKAP scaffolds in defined, serum-free culture media were placed in hydrogel (0.15% puramatrix; BD, Warsaw, Poland) and maintained subsequently in differentiation medium: DMEM/F12 + ITS (1:100; Gibco) + FBS (2%; Gibco) + cAMP (in the form of di-butyryl cAMP that allows the compound to penetrate through cell membrane, 100–300 μM; Sigma) + retinoic acid (RA, 0.5 μM; Sigma) + brain-derived neurotropic factor (BDNF, 10 ng/mL; Sigma) + laminin (10–50 μg/mL; Sigma). Half of medium was replaced every other day to maintain relatively stable level of

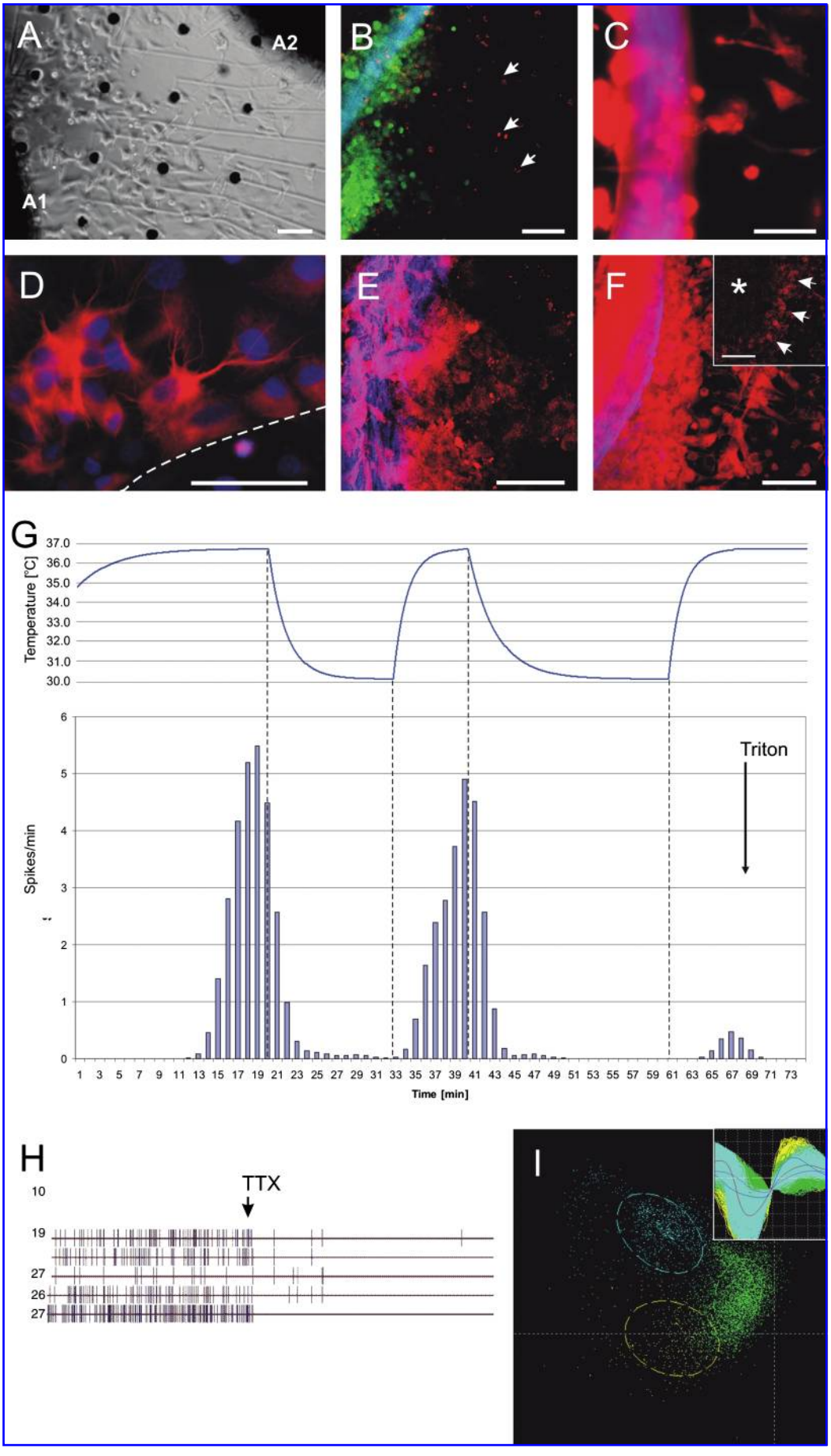
A
A2
A1
B
C
D
E
F
*
G
Temperature [°C]
37.0
36.0
35.0
34.0
33.0
32.0
31.0
30.0
Spikes/min
Triton
Time [min]
H
TTX
10
19
27
26
27
I

morphogenes (especially very sensitive RA). During 3 weeks of culture the stem cells migrate out of the attached aggregates and differentiate upon the area of multielectrode array (MEA) chips covered with electrodes, establishing there the neuronal network.

Electrophysiology

To record a field potential activity on the part of the neuronal network, aggregates were placed on poly-l-lysine–coated MEA chips (CMOS MEA, Bionas Measurement System[16], Rostock, Germany; glass MEA, Center for Network Neuroscience, University of Texas)[17] at the edges of a field covered with electrodes (Fig. 3A). The culture of HUCB-NSC has been performed on two types of MEA chips made on glass substrate with ITO electrodes[18,19] and silicon MEAs where electrodes were made in complementary melal-oxide semiconductor technology (CMOS).[16,20] At the end of the third week of culture in differentiating medium electrophysiological screening of field potential has been performed and recorded with MEA setup composed of Bionas NI58 chip interface (for CMOS MEA) and CNN interface (type ORC-1) adapted by Bionas for glass MEA chips. Analog to digital conversion has been performed by 64-channel digitizer from Bionas. The sampling frequency was 20 kHz with 16-bit resolution. Online spike detection has been performed by adaptive thresholding. Measurements have been stored and processed on the PC with the Neuro Explorer™ software package from Plexon™, Dallas, TX. To asses the neuronal activity, several parameters, such as spike rate (number of spikes per second), burst rate (number of bursts per second), inter spike/burst interval, have been extracted from the activity recordings.

Transmission electron microscopy

For morphological ultrastructural studies, the aggregates of NSC derived from HUCB-NSC that grow based on HKAP scaffolds in defined, serum-free culture media were fixed with Karnovsky solution (2% paraformaldehyde and 2.5% glutaraldehyde in 0.2 M sodium cacodylate buffer, pH 7.4, for 2 h at room temperature), washed in the same buffer lacking the fixative, and post-fixed in 1% osmium tetroxide for 1 h. The aggregates were dehydrated through serial incubation in graded series of acetone solutions (30%, 60%, 90%, and 100%) and finally embedded in Epon. The blocks were cut with LKB-Nova microtome, and the sections were counter-stained with uranyl acetate and lead citrate, and examined with a JEOL EX electron microscope at 80 kV.

mRNA expression analysis

Total RNA was isolated using the RNAeasy mini-kit (Qiagen, West Sussex, United Kingdom) from free-floating aggregates of HUCB-NSC based on HKAP scaffolds. Reverse transcription was made in 20 μL of reactions using 1 μg of RNA per reaction heated at 65°C cDNA with 1 μg of oligo-dT for 2 min. Samples were cooled on ice and mixed with 200 units of SuperScript Rnase H^- Reverse Transcriptase (Invitrogen, Paisley, United Kingdom) in its associated buffer, 400 μM of dNTPs (Amersham Biosciences, Buckinghamshire, United Kingdom) and 40 units of RNAseout (Invitrogen). Then, samples were incubated at 37°C for 1 h for 10 min and finally heated at 70°C for 15 min. PCR reaction was carried out in a 25 μL reaction using 1U Taq DNA Polymerase (Fermentas, York, United Kingdom) using an identical amount of cDNA per reaction with 1 μM of forward (F) and reverse (R) primers, respectively. Following primers were used: Oct4: 5′-CTCTGA GGAGTGGGGGATTC-3′; 5′-TTGTGCATAGCCACTGCTTG-3′; Rex1 5′-CAGATCCTAAACAGCTCGCAGAAT-3′; 5′-GCG TACGCAAATTAAAGTCCAGA-3′; SOX2: 5′-AGTCTCCAA GCGACGAAAAA-3′; 5′-GGAAAGTTGGGATCGAACAA-3′; Nestin: 5′-AGGATGTGGAGGTAGTGAGA-3′; 5′-TGGAGA TCTCAGTGGCTCTT-3′; GAPDH: 5′-TGAAGGTCGGAGTC AACGGATTTGG-3′; 5′-CATGTAGGCCATGAGGTCCACC AC-3′. PCR products were separated by electrophoresis on 1% agarose gel in 0.5×TBE buffer and visualized by ethidium bromide staining. Gel images were acquired with a GelExpert 4.0.

Immunocytochemical validation

Aggregates previously fixed with 4% PFA were blocked and permeabilized with 5% normal goat serum (Sigma) mixed with 0.1% Triton X-100 for 60 min at RT. Subsequently, primary antibodies were applied: mouse monoclonal IgG1 against Ki67 (Novocastra, Newcastle Upon Tyne, United Kingdom), mouse monoclonal IgG1 against MAP2 (Sigma), mouse monoclonal IgG1 against Connexin 43 (Chemicon), mouse monoclonal IgG1 against NF200 (Sigma), goat polyclonal IgG against GFAP (Dako, Glostrup, Denmark), and goat polyclonal IgG against S100β (Swant, Bellinzona, Switzerland). After washing with PBS, the secondary antibodies conjugated with Alexa 594 or Alexa 488 fluorochromes (Invitrogen) were applied for 60 min at RT. Cell nuclei were stained with 5 μM Hoechst 33258 (Sigma) for 20 min. After the final wash the slides were mounted in Fluoromount-G (Southern Biotechnology Association, Galveston, TX). As a control, first antibodies were omitted during immunocytochemistry staining. To obtain detailed images of the cells, a

FIG. 3. Functional neural circuits generated from HUCB-NSC. Scaffold-based aggregates were placed on MEA chip electrodes (black dots), and upon differentiation functional connective neuronal network was formed between two aggregates A1 and A2 (**A**). During differentiation, proliferative Ki67+ (red) neuroblasts migrate out from the aggregate (**B**, arrows) and differentiate toward functional neurones that expressed TUJ1 (**D**, red), GABA-associated protein (**E**, red), and MAP2 (**F**, red). Differentiation occurred preferably outside the niche-like aggregates (**F**, inset—confocal scanning of MAP2+ cells; arrows mark border of the niche indicated by the asterisk). Some of the HUCB-NSC differentiated toward astrocytes S100β+ (**C**). HKAP scaffolds were labeled blue (**B, C, E, F**) or marked by dotted line (**D**). Temperature-dependent modulation of the spike rate indicates neuronal spontaneous activity (field potential) inhibited permanently by triton X-100 (**G**). The raster plot displays the spontaneous spike action potential activity that is inhibited by TTX treatment (**H**). Interacting signals from at least three independent neurons were recognized on single MEA chip; sets of electrical activity readings from each neuron are indicated by different colors (**I**). Scale bars: 50 μm (**A–F**).

confocal laser scanning microscope (Zeiss LSM 510; Carl Zeiss, Oberkochen, Germany) was used. Following acquisition, images were processed using Zeiss LSM 510 software package v.2.8 and Corel Draw 11.

Results

Generation of 3D neural niches from HUCB-NSC

In our study we used stable NSC line derived from HUCB-NSC.[13] For generation of 3D neural organoids we obtained highly homogenous population of floating multipotent HUCB-NSC characterized elsewhere, which expressed Nestin (96%) and GFAP (40%).[12] Such floating HUCB-NSC were cocultured with scaffolds produced from HKAP in defined serum-free medium supplemented with EGF (20 ng/mL). For this study we chose HKAP scaffolds at different sizes ranging from 30 μm to 10 mm in length and average diameter of 50 μm. Surface of HKAP scaffolds promoted NSC adhesion and their subsequent tight connections that could be observed in microphotographs (Fig. 1J) of transmission electron microscopy (TEM). Within 3 weeks of coculture, HUCB-NSC formed a multilayer surface around the HKAP scaffolds, and such structures were transferred subsequently to new flasks to remove nonattached floating cells (Fig. 1E). During this time some of HUCB-NSC present within aggregates began to differentiate preferably toward neuronal phenotypes (Fig. 1A, B). We did not observe significant increase of astrocytes number depending on time or high passage of HUCB-NSC used for experiments. Such scaffold-based aggregates comprised multipotent NSC as well as their progeny at various stages of neural differentiation. Analysis of mRNA level revealed expression of transcription factors involved in maintenance of stem cell pluripotency (*Oct4* and *Sox2*) and neural lineage commitment (*Rex1* and *Nestin*) (Fig. 2). Confocal analysis of the aggregate structure showed that NSC situated in the core of the aggregates—proximal to the scaffold—remain undifferentiated and display mitotic activity (Ki67+) (Fig. 1D). Besides multipotent NSC, also more mature neural phenotypes appeared preferably on the surface of HKAP scaffolds, for example, NF200, MAP2, or S100β (Fig. 1A–C, respectively). Most of the cells in the aggregate were connected with gap junctions and expressed their marker protein connexin 43 (Fig. 1F). Microphotographs from TEM analysis showed gap and tight junction between NSC present in the aggregate (Fig. 1I). We found that HKAP scaffolds were easily digested by surrounded cells without any signs of toxicity or increased apoptosis (Fig. 1G, H). It is noteworthy that spontaneously formed aggregates without supporting HKAP scaffolds did not undergo niche-like cellular stratification and did not form tightly connected structures as described previously.[12]

Maturation of artificial neural tissue

Aggregation of HUCB-NSC on HKAP scaffolds facilitates differentiation of neural progenitors in the presence of morphogenes, and concomitantly maintains the proliferation and migration of less-differentiated NSC from their reservoir localized in the core of the aggregate (Fig. 3A, B). We observed that HUCB-NSC situated at the surface of the aggregate underwent very rapid differentiation (up to 1 week)—preferentially into neuronal phenotypes—in the presence of inductive signals such as di-butyryl cyclic AMP (dBcAMP), BDNF, and all-trans RA (Fig. 3F). The embedding of scaffold-based HUCB-NSC aggregates with ECM proteins (laminin or puramatrix) facilitates NSC migration out of the aggregate, as well as improved their further differentiation and formation of neuronal circuits. During differentiation, neuroblasts (TUJ1+ and Ki67+) were migrating out the niche and spread their processes within surrounded hydrogel (puramatrix), which stiffness matched this observed in neural tissue (0.1–0.15% protein content). The confocal analysis revealed proliferating (Ki67+) HUCB-NSC neuroblasts both inside and outside the central region of the attached aggregate (niche), after 3 weeks since differentiation began (Fig. 3A, B). In contrast, Nestin+/GFAP+/Ki67−NSCs were located within the aggregate, proximal to the remnants of the protein scaffold. Most of the migrating neuroblasts differentiated into neurones expressing β-tubulin III (TUJ1), NF200, and MAP2, and constituting a network outside the niche (Fig. 3A, D–F). However, some of the HUCB-NSC generated astroglia (S100β+) (Fig. 3C).

Functional properties of neuronal network

During the process of differentiation (3 weeks) NSC were migrating out from the attached aggregates and ultimately formed a neuronal network (described above) upon the surface covered with electrodes (Fig. 3A). We found that such a network was able to generate spontaneous activity after 3 weeks of culture in differentiation-promoting medium containing RA, cAMP, BDNF, and dissolved laminin (Fig. 3G). Field potential activity was recorded by single electrodes just after the second week of differentiation. At the end of third week of culture, 16% (9 out of 55) of the investigated chips showed spontaneous activity, with approximately 11 firing neurons proving detectable on each active MEA chip (Fig. 3G, H). This was approximately 10 times more active neurones comparing to HUCB-NSC cultured in two-dimensional (2D) monolayer. It is worth to stress that analysis of such firings revealed some being generated sequentially, in response to earlier firing from other ones present in 3D network (Fig. 3I). This spontaneous network activity could be blocked reversibly by TTX treatment or low temperature (Fig. 1G and 1H, respectively), thereby further attesting to the presence of an action potential in differentiated HUCB-NSC.

Discussion

As transplantation medicine suffers from lack of organ donors, stem cell–based regenerative medicine got broad choice of sources of pluripotent stem cells; however, their potential for clinical application still needs to be evaluated. Important issue arising where the clinical application is concerned would be the safety and functionality of the recruitment. Regarding this criteria we decided to test HUCB-NCS for their potential to generate an artificial neural tissue *in vitro*. Recently, cord blood stem cells have become one of the most promising tools for stem cell–based regenerative therapy when considering their safety, accessibility, low cost, and broad differentiation potential. HUCB cells are easily accessible from cord blood banks, and further isolation of pluripotent SC has been reported worldwide and requires a minimum of reagents and equipments.[21–23]

However, the exact mechanisms underlying the prolonged proliferation of pluripotent stem cells isolated from HUCB and their differentiation toward functional neurons need to be elucidated as a matter of priority if the procedures are to be standardized.

We previously characterized a number of voltage-sensitive and ligand-gated channels in 2D monolayer cultures of HUCB-NSC.[24] However, such cells were not performed electrical activity characteristic for functional neuronal circuits. It is known that cell–cell interactions and generation of physic-chemical microenvironments within developing tissue are critical factors for proper development of functional brain tissue.[25,26] Recently, we found that differentiation of NSC highly depends on cell–cell interactions in a 3D environment. We described that NSC that were transplanted on hippocampal organotypic slices differentiated more rapidly and gained more advanced morphology than NSC grown in 2D cultures.[12,27] The physiological hallmark of formation of tissue-like structure is generation of gap junctions between the cells. Cell–cell interactions revealed by gap junction appearance play a crucial role in development of CNS.[28] In NSC niches, cell–cell interactions and ECM are described as a critical factors support NSC survival, growth rate, and symmetry as well as differentiation.[29] Therefore, in this study to initiate cell aggregation we used scaffolding material and culture medium containing dissolved ECM proteins (e.g., laminin and fibronectin). We observed that surface of 3D HKAP scaffolds becomes attractive to NSC and promotes higher neuronal differentiation than 2D culture systems of HUCB-NSC.[12,13] For clinical perspective, application of human-derived scaffolds is very promising in terms of their low immunogenity and fast biodegradation. This method raises also the possibility of particular substances being encapsulated in the protein scaffold and then delivered into the CNS with a view to support proliferation and survival/differentiation of endogenous and/or grafted NSC.[15] HKAP scaffolds seem to improve significantly cell differentiation or lesion repair, as it was shown in cartilage, bone, skin, or liver regeneration.[30] This opens up alongside the possibility of the scaffold-based aggregates being used in the differentiation of the other types of pluripotent cells from HUCB (or other sources) toward liver, bone, cartilage, or other tissue, in line with the broad developmental potential attributed to HUCB stem cells.[23]

This work shows that the 3D environment is very important for development of functional neurones *in vitro*. Neuronal maturation depends on different morphogenes (e.g., BDNF and RA), which must be introduced in a time-specific manner. However, final differentiation of neural tissue revealed by its functional properties requires cell–cell interactions in a 3D environment. In this study we focused on investigating functional properties of the artificial neural tissue as a whole rather than analysis of a single-cell neuronal activity. Traditionally, voltage- or current-patch clamp or voltage-sensitive dyes have been used to directly measure the currents generated by action potentials in neurons.[31,32] Although very sensitive, these methods are highly localized, invasive, and often very difficult to perform routinely and reproducibly. As an alternative approach, extracellular recordings of action potentials have been proposed.[33,34] Fluctuations in electrical field potential associated with current flow can be measured by employing an MEA embedded on planar substrate with neural culture on it.[17,35] Additional advantage of the MEA approach over traditional methods is possibility to perform long-term recordings and stimulations and mapping the activity of a network of cultured neurons in both space and time. Therefore, currently, MEA evolved into a reliable platform with significant contributions to the fields of neuroscience and biosensing.[36] Our experiment revealed that dissociated aggregates and HUCB-NSC in 2D culture systems, where cell–cell interaction were disrupted, did not reveal network-like appearance in comparison to 3D HKAP-based artificial neural tissue. According to our recent experiments niche-like 3D structures resembling functional brain tissue are very promising model systems for *in vitro* study of neural plasticity. The results of our work presented here indicate that HUCB is a good source of stem cells capable of crossing tissue boundaries and differentiating into functional neurones in 3D culture systems.

Acknowledgments

Financial support from the Polish Ministry of Sciences and High Educations via Grants 0141/B/P01/2008/35, NN401014235, and 3TO/9B/03029, and JRC Enlargement and Integration Project, European Commission, is acknowledged.

Disclosure Statement

No competing financial interests exist.

References

1. Bliss, T., Guzman, R., Daadi, M., and Steinberg, G.K. Cell transplantation therapy for stroke. Stroke **38,** 817, 2007.
2. Buhnemann, C., Scholz, A., Bernreuther, C., Malik, C.Y., Braun, H., Schachner, M., Reymann, K.G., and Dihne, M. Neuronal differentiation of transplanted embryonic stem cell-derived precursors in stroke lesions of adult rats. Brain **129,** 3238, 2006.
3. Liste, I., Garcia-Garcia, E., and Martinez-Serrano, A. The generation of dopaminergic neurons by human neural stem cells is enhanced by Bcl-XL, both *in vitro* and *in vivo*. J Neurosci **24,** 10786, 2004.
4. Sun, J., Gao, Q., Miller, K., Wang, X., Wang, J., Liu, W., Bao, L., Zhang, J., Zhang, L., Poon, W.S., and Gao, Y. Dopaminergic differentiation of grafted GFP transgenic neuroepithelial stem cells in the brain of a rat model of Parkinson's disease. Neurosci Lett **420,** 23, 2007.
5. Willing, A.E., Lixian, J., Milliken, M., Poulos, S., Zigova, T., Song, S., Hart, C., Sanchez-Ramos, J., and Sanberg, P.R. Intravenous versus intrastriatal cord blood administration in a rodent model of stroke. J Neurosci Res **1,** 296, 2003.
6. Kozlowska, H., Jablonka, J., Janowski, M., Jurga, M., Kossut, M., and Domanska-Janik, K. Transplantation of a novel human cord blood-derived neural-like stem cell line in a rat model of cortical infarct. Stem Cells Dev **16,** 481, 2007.
7. Nan, Z., Grande, A., Sanberg, C.D., Sanberg, P.R., and Low, W.C. Infusion of human umbilical cord blood ameliorates neurologic deficits in rats with hemorrhagic brain injury. Ann NY Acad Sci **1049,** 84, 2005.
8. Park, K.I., Teng, Y.D., and Snyder, E.Y. The injured brain interacts reciprocally with neural stem cells supported by scaffolds to reconstitute lost tissue. Nat Biotechnol **20,** 1111, 2002.
9. Zigova, T., Song, S., Willing, A.E., Hudson, J.E., Newman, M.B., Saporta, S., Sanchez-Ramos, J., and Sanberg, P.R.

Human umbilical cord blood cells express neural antigens after transplantation into the developing rat brain. Cell Transplant **11,** 265, 2002.
10. Buzanska, L., Machaj, E.K., Zablocka, B., Pojda, Z., and Domanska-Janik, K. Human cord blood-derived cells attain neuronal and glial features *in vitro*. J Cell Sci **115,** 2131, 2002.
11. Kang, K.S., Kim, S.W., Oh, Y.H., Yu, J.W., Kim, K.Y., Park, H.K., Song, C.H., and Han, H. A 37-year-old spinal cord-injured female patient, transplanted of multipotent stem cells from human UC blood, with improved sensory perception and mobility, both functionally and morphologically: a case study. Cytotherapy **7,** 368, 2005.
12. Jurga, M., Markiewicz, I., Sarnowska, A., Habich, A., Kozlowska, H., Lukomska, B., Buzanska, L., and Domanska-Janik, K. Neurogenic potential of human umbilical cord blood–neural-like stem cells depends on their previous long-term culture conditions. J Neurosci Res **83,** 627, 2006.
13. Buzanska, L., Jurga, M., Stachowiak, E.K., Stachowiak, M.K., and Domanska-Janik, K. Neural stem-like cell line derived from a nonhematopoietic population of human umbilical cord blood. Stem Cells Dev **15,** 391, 2006.
14. Cho, M.S., Lee, Y.E., Kim, J.Y., Chung, S., Cho, Y.H., Kim, D.S., Kang, S.M., Lee, H., Kim, M.H., Kim, J.H., Leem, J.W., Oh, S.K., Choi, Y.M., Hwang, D.Y., Chang, J.W., and Kim, D.W. Highly efficient and large-scale generation of functional dopamine neurons from human embryonic stem cells. Proc Natl Acad Sci USA **4,** 3392, 2008.
15. Lipkowski, A.W., Jurga, M., Domanska-Janik, K., and Lukomska, B. New protein scaffolds and methods of their preparation and applications. Polish Pat Appl P380011, 2006.
16. Krause, G., Lehmann, M., Freund, I., Schreiber, E., Weiss, D.G., and Baumann, W. Measurement of electrical activity of long-term mammalian neuronal networks on semiconductor neurosensor chips and comparison with conventional microelectrode arrays. Biosens Bioelectron **21,** 1272, 2006.
17. Gross, G., Rhoades, B.K., Azzazy, H.M.E., and Ming Chi, W. The use of neuronal networks on multielectrode arrays as biosensors. Biososen Bioelectron **10,** 553, 1995.
18. Gross, G.W., Wen, W., and Lin, J. Transparent indium-tin oxide patterns for extracellular, multisite recording in neuronal cultures. J Neurosci Methods **15,** 243, 1985.
19. Lucas, J.H., Kirkpatrick, J.B., and Gross, G.W. A photoetched matrix for cell relocation in culture and histology. J Neurosci Methods **14,** 211, 1985.
20. Heer, F., Franks, W., Blau, A., Taschini, S., Ziegler, C., Hierlemann, A., and Baltes, H. CMOS microelectrode array for the monitoring of electrogenic cells. Biosens Bioelectron **2,** 358, 2004.
21. Ende, M., and Ende, N. Hematopoietic transplantation by means of fetal (cord) blood. A new method. Va Med Mon **99,** 276, 1972.
22. Habich, A., Jurga, M., Markiewicz, I., Lukomska, B., Bany-Laszewicz, U., and Domanska-Janik, K. Early appearance of neural progenitors in human cord blood mononuclear cells cultured *in vitro*. Exp Hematol **34,** 914, 2005.
23. McGuckin, C.P., Forraz, N., Baradez, M.O., Navran, S., Zhao, J., Urban, R., Tilton, R., and Denner, L. Production of stem cells with embryonic characteristics from human umbilical cord blood. Cell Prolif **38,** 245, 2005.
24. Sun, W., Buzanska, L., Domanska-Janik, K., Salvi, R.J., and Stachowiak, M.K. Voltage-sensitive and ligand-gated channels in differentiating neural stem-like cells derived from the nonhematopoietic fraction of human umbilical cord blood. Stem Cells **23,** 931, 2005.
25. Leone, D.P., Relvas, J.B., Campos, L.S., Hemmi, S., Brakebusch, C., Fässler, R., Ffrench-Constant, C., and Suter, U. Regulation of neural progenitor proliferation and survival by β1 integrins. J Cell Sci **15,** 2589, 2005.
26. Ma, W., Tavakoli, T., Chen, S., Maric, D., Liu, J.L., O'Shaughnessy, T.J., and Barker, J.L. Reconstruction of functional cortical-like tissues from neural stem and progenitor cells. Tissue Eng Part A **14,** 1673, 2008.
27. Sarnowska, A., Jurga, M., Filipkowski, R.K., Duniec, K., and Domanska-Janik, K. Bilateral interaction between cord blood-derived human neural stem cells and organotypic rat hippocampal culture, December 3, 2008 (In press).
28. Sutor, B. Gap junctions and their implications for neurogenesis and maturation of synaptic circuitry in the developing neocortex. Results Probl Cell Differ **39,** 53, 2002.
29. Lin, H. The stem-cell niche theory: lessons from flies. Nat Rev Genet **3,** 931, 2002.
30. Lipkowski, A.W., Grabowska, A., Kurzepa, K., and Szczucinska, A. New microstructural protein preparations with adsorbed biological active substances and their applications in medicine and cosmetics. Polish Pat Appl P381103, 2006.
31. Gurkiewicz, M., and Korngreen, A. A numerical approach to ion channel modelling using whole-cell voltage-clamp recordings and a genetic algorithm. PLoS Comput Biol **3,** 169, 2007.
32. Zhou, W.L., Yan, P., Wuskell, J.P., Loew, L.M., and Antic, S.D. Intracellular long-wavelength voltage-sensitive dyes for studying the dynamics of action potentials in axons and thin dendrites. J Neurosci Methods **164,** 225, 2007.
33. Gross, G.W. Simultaneous single unit recording *in vitro* with a photoetched laser deinsulated gold multimicroelectrode surface. IEEE Trans Biomed Eng **5,** 273, 1979.
34. Regehr, W.G., Pine, J., Cohan, C.S., Mischke, M.D., and Tank, D.W. Sealing cultured invertebrate neurons to embedded dish electrodes facilitates long-term stimulation and recording. J Neurosci Methods **30,** 91, 1989.
35. Buitenweg, J.R., Rutten, W.L.C., Marani, E., Polman, S.K.L., and Ursum, J. Extracellular detection of active membrane currents in the neuron–electrode interface. J Neurosci Methods **2,** 211, 2002.
36. Pancrazio, J.J., Whelan, J.P., Borkholder, D.A., Ma, W., and Stenger, D.A. Development and application of cell-based biosensors. Ann Biomed Eng **27,** 687, 1999.

Address correspondence to:
Marcin Jurga, Ph.D.
Department of Neurorepair
Medical Research Institute
Polish Academy of Sciences
Warsaw 02-106
Poland

E-mail: jurgamarcin@gmail.com

Received: August 27, 2008
Accepted: November 21, 2008
Online Publication Date: January 27, 2009